

INJECTION REGION PROBING BY BEAM AT VEPP-2000 STORAGE RING

D. Shwartz^{†1}, I. Koop¹, E. Perevedentsev¹, Yu. Rogovsky¹, M. Timoshenko,
Budker Institute of Nuclear Physics, Novosibirsk, 630090, Russia
¹also at Novosibirsk State University, Novosibirsk, 630090, Russia

Abstract

VEPP-2000 electron-positron collider for multiple injection and stacking uses traditional scheme with pre-kicker, kicker and pulsed thin septum magnet. It was found earlier that despite the shielding septum stray field disturbs the circulating beam and sweeps its betatron tune long after the magnet pulse. This work presents the beam-based measurements of mechanical aperture at the interaction region and discusses stray field mapping technique.

INTRODUCTION

During VEPP-2000 commissioning phase the observation was done that circulating beams are disturbed by weak leakage fields of pulsed septum magnet ME5. The typical pickup signal from the beam disturbed by septum stray field is shown in Fig. 1. The time of full-sine magnet driving pulse corresponds to $280 \mu\text{s} / 82 \text{ ns} = 3400$ turns (shown with green zone). One can see that stray field has much longer decay time.

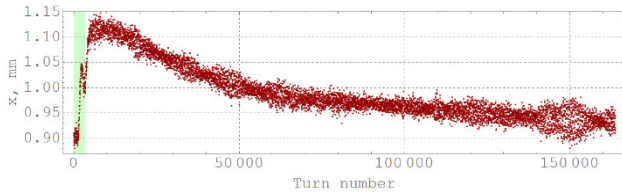


Figure 1: Beam closed orbit distortion observed by pickup.

Finally, it was proposed to make beam-based measurements of septa stray fields.

VEPP-2000 OVERVIEW

VEPP-2000 storage ring description and basic parameters can be found elsewhere [1-6]. It is a small 24 m perimeter single-ring electron-positron collider with energy range of 150-1000 MeV per beam. It operates with round beams and uses solenoids for final focusing [7].

The injection scheme [8] is dictated by very tight room. Although the additional powerful pulsed magnet (ME4/MP4, see Fig. 2) is introduced to relax the septum magnet ME5/MP5, the latter should produce field over 20 kGs for injection at collider top energy of 1 GeV.

VEPP-2000 BPM system is based on 16 CCD matrices reading beam profiles via synchrotron radiation (SR) outputs from each edge of dipoles (see blue and red dots in Fig. 2) [9].

For pulsed closed orbit (CO) distortions only the fast pickup BPMs are useful. VEPP-2000 storage ring is

equipped with only 4 pickups [10]. Each pickup works either in slow CO measurement regime or in external trigger regime when electronics captures the set of turn-by-turn data.

The schematic layout of the VEPP-2000 collider is presented in Fig. 2. The points of SR output for electron and positron beams are shown with blue and red. Green marks show the arrangement of pickups.

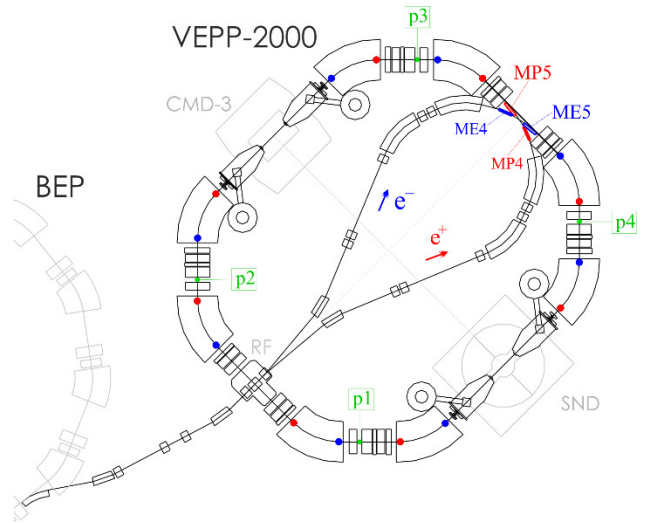


Figure 2: VEPP-2000 storage ring layout.

Septum Magnet Design

The septum magnet is an eddy-current type magnet with full-sine driving current pulse (see Fig. 3). The pulse rising time is $T/4 = 70 \mu\text{s}$, the current amplitude is up to 40 kA. The septum knife thickness is 2.5 mm and it includes 0.5 mm ferromagnetic shield introduced to suppress leakage field in circulating beam vacuum chamber.

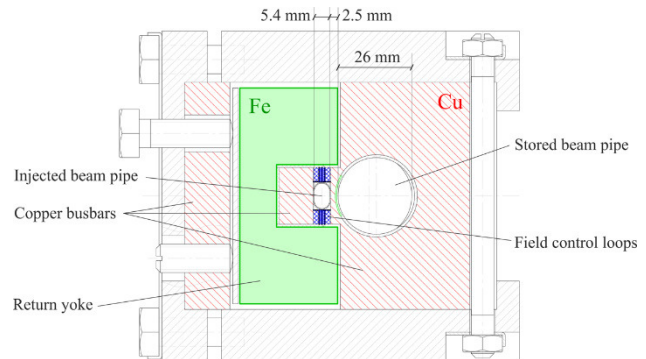


Figure 3: Septum magnet cross section. Red hatched area corresponds to copper components: bus bars and knife. With green are shown iron return yoke and shielding.

[†] d.b.shwartz@inp.nsk.su

BEAM ORBIT CONTROL

In order to use circulating beam as a probe one should variate and precisely control the beam CO at the region of disturbing field. Model-based CO distortions in two planes used for probing are shown in Fig. 4.

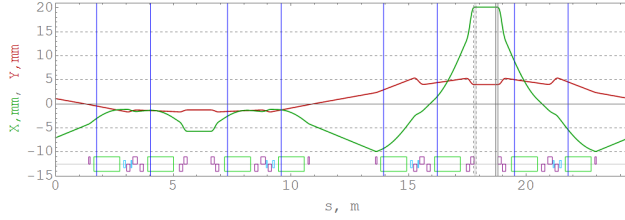


Figure 4: Horizontal (green) and vertical (red) CO distortion used for injection region probing. Blue lines indicate position of BPMs. Solid/dashed grey stripe shows the ME5/MP5 position.

The static orbit distortion is controlled by CCD-based BPMs. Usually the single-beam regime is used for these experiments thus 8 BPMs are available for CO control. The pattern of CO distortion is taken from the lattice model and compared to vector of 8 measured shifts.

In Fig. 5 CO distortion fit examples are presented: a) measured (points) and fitted (line) horizontal response of 8 BPMs; b) vertical response with three last BPMs lost the beam image due to very large CO shift.

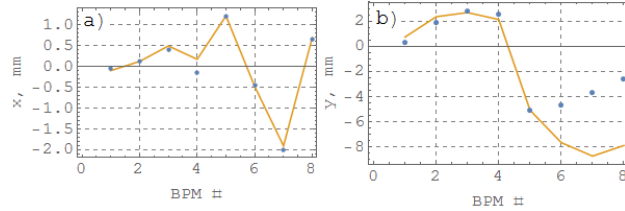


Figure 5: Closed orbit distortions samples.

Once the measured vector is fitted the CO coordinate is reconstructed at the desired position (e.g. septum magnet region) from the model. The residual between measured and best-fit model vectors is used to estimate the inaccuracy (systematic) of coordinate control. Unfortunately for very large orbit shifts significant discrepancy between model and measured patterns appears (see later in Fig. 7). The first-order correction of linear model with known sources of nonlinear fields (chromatic sextupoles) only partially explain this discrepancy.

We should mention that prior to beam-based and model-dependent measurements the routine orbit and linear lattice corrections based on orbit response matrix SVD-analysis are done [11].

PROBING THE APERTURE

In order to crosscheck the accuracy of large coordinate shift another approach was used. The tests were carried out at relatively low energy of 340 MeV where the beam lifetime is typically restricted by Touschek effect for any beam intensities acceptable for pickup reliable operation (> 1 mA). At the same time with the limited horizontal aperture A_x , the elastic scattering on the nuclei of rest gas

comes into play. For the very small aperture $\sim 4-5 \sigma$ of beamsizes the quantum lifetime gives the limit. Thus, measurement of the lifetime τ with respect to orbit shift while approaching the known aperture limit can be used for coordinate calibration.

In presence of transverse aperture limitation the inverse beam lifetime can be written as a sum of two components:

$$\frac{1}{\tau} = \frac{1}{\tau_{qu}} + \frac{1}{\tau_{el}}. \quad (1)$$

The lifetime driven by elastic scattering τ_{el} is proportional to square of aperture [12] thus can be expressed as:

$$\tau_{el} = \frac{A_x^2}{\alpha}, \quad (2)$$

where α coefficient depends on gas pressure and machine lattice functions. The quantum lifetime τ_{qu} has a very sharp dependence on the aperture limitation [13]:

$$\tau_{qu} = \tau_d \frac{\sigma_x^2}{A_x^2} e^{\frac{A_x^2}{2\sigma_x^2}}. \quad (3)$$

Here $\tau_d = 90$ ms is damping time, $\sigma_x = 0.35$ mm is horizontal beamsizes at the aperture limitation region. Both this parameters are known from model. Beamsizes additionally controlled at all CCDs to be in accordance with model. We will fit measured lifetime with a combination of two components with single aperture limit x_0 .

$$\frac{1}{\tau} = \frac{1}{\tau_d} \frac{(x - x_0)^2}{\sigma_x^2} e^{-\frac{(x - x_0)^2}{2\sigma_x^2}} + \frac{\alpha}{(x - x_0)^2}. \quad (4)$$

In Fig. 6 the measured lifetime dependence is presented together with fit result.

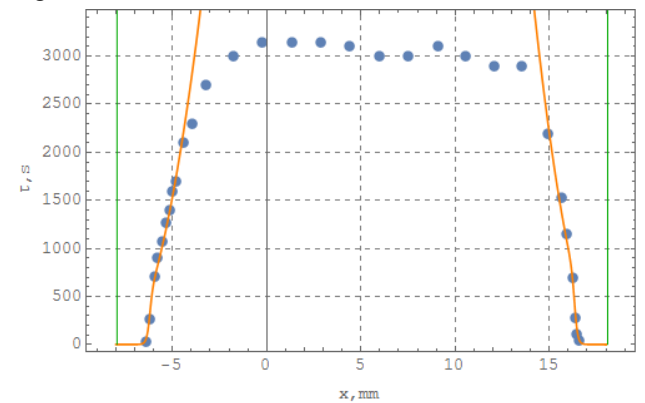


Figure 6: Measured (points) and fitted (yellow lines) beam lifetime as a function of horizontal coordinate. Green lines indicate the position of obtained aperture limit.

The reconstructed from fit positions of mechanic aperture corresponds to $x_0 = -7.9$ mm, $x_0 = +18.1$ mm. Sum of

these values gives the horizontal gap of 26 mm being in good agreement with design (see Fig. 3). This agreement indicates that coordinate errors obtained from coordinate reconstruction procedure are overestimated.

STRAY FIELD MEASUREMENTS

To measure pulsed stray field we analyze the signals from all 4 pickups (see Fig. 1) and average the data over ~ 1000 turns near the maximum of orbit shift. The response measured by four pickups \vec{x}_{exp} , \vec{y}_{exp} is compared with model vector of four components and fitted amplitude gives the integral of disturbing field.

Response fitting example is presented in Fig. 7. Points and lines are for measured and fitted CO shifts, correspondingly. Blue and purple are for horizontal and vertical responses.

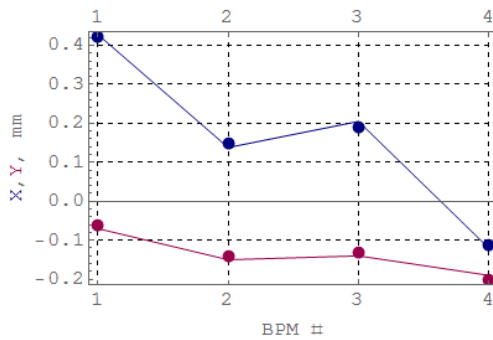


Figure 7: Response fitting example.

The stray field of two different magnets ME5, MP5 was measured at the driving pulse level nominal for injection at 340 MeV. The resulting stray field dependencies on horizontal coordinate are presented in Fig. 8. These two injection septa for electron and positron beams correspondingly have identical design and both powered by single power converter with mechanical commutator.

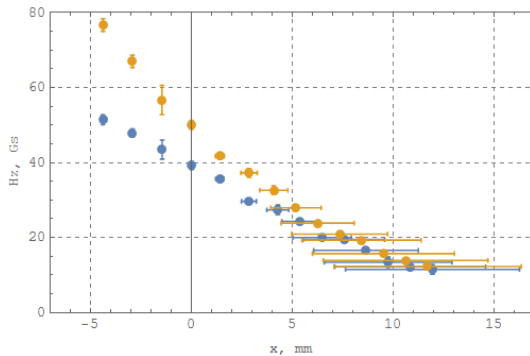


Figure 8: Stray fields of ME5 (blue), MP5 (yellow) dependence on horizontal coordinate. Here we assume the length of disturbing field region equal to 10 cm.

Error bars here indicate the (over)estimation of systematic inaccuracy of the field and coordinate reconstruction obtained from discrepancy of model and measured closed orbit distortion.

Leakage field of ME5 septum magnet at the regular CO dependence on driving pulse amplitude is presented in Fig. 9. Vertical green lines marks the two levels corresponding to 340 and 910 MeV beam injection energy.

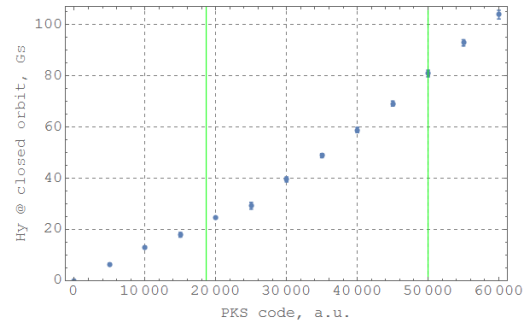


Figure 9: Field at CO dependence on driving pulse amplitude.

Although the dependence is nonlinear the significant slope at low current indicates that leakage is not explained by saturation of thin magnetic shield.

CONCLUSION

We have shown that circulating beam can be used as a sensitive and convenient instrument for field mapping. Beam-based method allows to measure pulsed fields inside the vacuum chamber of assembled and operating machine. The stray field of VEPP-2000 septum magnets was measured.

ACKNOWLEDGEMENT

We are grateful to D. E. Berkaev, B. Z. Persov, V. P. Prosvetov and Yu. M. Zharinov for support with pulsed septum design and operation. We would like to thank A. L. Romanov and A. I. Senchenko for assistance in orbit responses technique software.

REFERENCES

- [1] Yu.M. Shatunov *et al.*, "Project of a New Electron-Positron Collider VEPP-2000", in *Proc. EPAC'00*, Vienna, Austria, 2000, pp. 439-441.
- [2] D. E. Berkaev *et al.*, "The VEPP-2000 electron-positron collider: First experiments", *J. Exp. Theor. Phys.*, Vol.113, no.2, p.213 (2011)
- [3] P. Yu. Shatunov *et al.*, "Status and perspectives of the VEPP-2000", *Phys. Part. Nucl. Lett.* (2016) v.13, no.7, pp. 995-1001.
- [4] D. Schwartz *et al.*, "Implementation of Round Colliding Beams Concept at VEPP-2000", in *Proc. eeFACT'16*, Daresbury, UK (2016), p. 32.
- [5] Yu. M. Shatunov *et al.*, "Commissioning of the Electron-Positron Collider VEPP-2000 after the Upgrade", *Phys. Part. Nucl. Lett.* (2018) v.15, no.3, pp. 310-314.
- [6] D. Schwartz *et al.*, "Round Colliding Beams at VEPP-2000 with Extreme Tunes", in *Proc. eeFACT'18*, Hong Kong, China (2018), MOYBA01.
- [7] V.V. Danilov *et al.*, "The Concept of Round Colliding Beams", in *Proc. EPAC'96*, Sitges, Spain, 1996, pp. 1149-1151.

- [8] D. E. Berkaev *et al.*, "Beams Injection System for e^+e^- Collider VEPP-2000", in *Proc. EPAC'06*, Edinburgh, Scotland (2006), p.622.
- [9] Yu. A. Rogovsky *et al.*, "Beam Measurements with Visible Synchrotron Light at VEPP-2000 Collider", in *Proc. DIPAC'11*, Hamburg, Germany (2011), p. 140.
- [10] Yu. A. Rogovsky *et al.*, "Pickup Beam Measurement System at the VEPP-2000 Collider", in *Proc. RuPAC'10*, Protvino, Russia (2010), p. 101.
- [11] A.L. Romanov *et al.*, "Round Beam Lattice Correction using Response Matrix at VEPP-2000", in *Proc. IPAC'10*, Kyoto, Japan, 2010, pp. 4542-4544.
- [12] J. Le Duff, "Current and Current Density Limitations in Electron Storage Rings", *Nucl. Instrum. Methods Phys. Res., Sect. A* 239, 83 (1985).
- [13] A. W. Chao, M. Tigner, "Handbook of Accelerator Physics and Engineering" (WorldScientific, Singapore, 1999), p.188.